

## Symplastic isolation of the sieve element-companion cell complex in the phloem of *Ricinus communis* and *Salix alba* stems

Aart J.E. van Bel and Ronald Kempers

Transport Physiology Research Group, University of Utrecht, Lange Nieuwstraat 106, NL-3512 PN Utrecht, The Netherlands

Received 2 May; accepted 21 July 1990

**Abstract.** The anatomical and physiological isolation of the sieve element-companion cell complex (se-cc complex) was investigated in stems of *Ricinus communis* L. and *Salix alba* L. In *Ricinus*, the plasmodesmatal frequencies were in the proportions 8:1:2:30, in the order given, at the interfaces between sieve tube-companion cell, sieve tube-phloem parenchyma cell, companion cell-phloem parenchyma cell, and phloem parenchyma cell-phloem parenchyma cell. The membrane potentials of the se-cc complex and the surrounding phloem-parenchyma cells sharply contrasted: the membrane potential of the se-cc complex was about twice as negative as that of the phloem parenchyma. Lucifer Yellow CH injected into the sieve element or into the companion cell remained within the se-cc complex. Dye introduced into phloem parenchyma only moved (mostly poorly) to other phloem-parenchyma cells. The distribution of the plasmodesmatal frequencies, the differential dye-coupling and the sharp discontinuities in membrane potentials indicate that the se-cc complexes constitute symplast domains in the stem phloem. Symplastic autonomy is discussed as a basic necessity for the functioning of the se-cc complex in the stem.

**Key words:** Iontophoresis – Phloem translocation – *Ricinus* – *Salix* – Sieve element-companion cell complex – Symplastic isolation

### Introduction

The chief function of sieve tubes is the translocation of photoassimilates from sources to sinks. In order to achieve maximal source-sink transfer, the concentration gradient in the sieve-tube system must be as steep as possible. This demand conflicts with the considerable solute leakage along the translocation path which has

been revealed by use of metabolic inhibitors (Wolswinkel and Ammerlaan 1983; Minchin and Thorpe 1984; Minchin et al. 1984; Hayes and Patrick 1985; Hayes et al. 1985, 1987; Minchin and Thorpe 1987). An active resorption system is thus required to maintain the solute concentration in the sieve tubes along the leaf veins, petioles and stems. The intense retrieval is probably energized by a high inward-directed proton-motive force generated by the sieve element-companion cell complex (se-cc complexes) ( $\Delta\text{pH}$  2–3, Giaquinta 1983; membrane potential ( $E_m$ ) –140 to –160 mV, Wright and Fisher 1981; Fromm and Eschrich 1988; Van der Schoot and Van Bel 1989). These values enable photosynthate accumulation by factors between  $10^4$  and  $10^6$ .

Such a pump-leak system would benefit from a symplastic isolation of the se-cc complexes, i.e. the se-cc complex is a symplast domain. Efficient resorption by the se-cc complex through carrier systems is difficult to reconcile with symplastic exchange of solutes with adjacent cells. Symplastic isolation would therefore be a meaningful adaption to pump-leak control of the sieve-tube content. The ultrastructure of the phloem of *Mimosa* (Esau 1973) and *Phaseolus* (Hayes et al. 1985) stems is indicative of symplastic isolation of the se-cc complex in stem phloem. Dye-coupling experiments and electrophysiological mapping of the phloem of tomato petioles and stems (Van der Schoot and Van Bel 1989, 1990) also hinted at symplastic isolation of the se-cc complex. More convincing evidence in support of the symplastic autonomy of the se-cc complex would be given by combined ultrastructural and physiological studies in the same species. This paper describes integrative ultrastructural, electrophysiological and dye-coupling studies on the se-cc complex in *Salix* and *Ricinus* stems.

### Material and methods

**Plant material.** Basal internodes were excised from two- to four-month-old *Ricinus communis* L. pot plants that were cultivated in a greenhouse under daylight conditions and temperatures be-

**Abbreviations:**  $E_m$  = membrane potential; LYCH = Lucifer Yellow CH; se-cc complex = sieve element-companion cell complex

tween 20 and 35°C. Small twigs (10–15 mm in diameter) were cut from willow trees (*Salix alba* L.) in the laboratory garden. Stem pieces of 60 mm in length were excised for experimentation.

**Transmission electron microscopy.** Pieces (3·3·5 mm<sup>3</sup>) of the phloem region were submersed in a fixative (100 mol·m<sup>-3</sup> sodium-cacodylate buffer, 2 mol·m<sup>-3</sup> CaCl<sub>2</sub>, 2 mol·m<sup>-3</sup> MgCl<sub>2</sub>, 2% paraformaldehyde and 2.5% glutaraldehyde, pH 6.8) and stored overnight at 4°C. The tissues were postfixed with 1% OsO<sub>4</sub> in sodium-cacodylate buffer for 1 h. After dehydration in a graded ethanol series the tissues were impregnated and embedded in Spurr's resin. Ultrathin sections were cut with a diamond knife on a Reichert (Vienna, Austria) UM3 ultramicrotome. The sections were contrasted with uranyl acetate in 70% ethanol for 5–10 min and with lead citrate for 2 min. The sections, supported by a Parlodion or Formvar film on 75-mesh grids, were viewed and photographed at 60 kV with a Philips (Eindhoven, the Netherlands) EM 300 electron microscope.

**Preparation of the phloem tissue for electrode impalement.** Two parallel longitudinal incisions were made in the stem surface and the bark between was torn off along the cambial interface. From the outside, a paradermal longitudinal cut was made with a very sharp razor blade in the middle of the strip. The slicing exposed a layer of the functional phloem. The strips were trimmed to a final size of 40·10 mm<sup>2</sup> and incubated in a standard medium in darkness at room temperature for 1–6 h or for 24–30 h (ageing). The standard medium contained 125 mol·m<sup>-3</sup> mannitol, 10 mol·m<sup>-3</sup> NaOH-Mes (2-(N-morpholino)ethanesulfonic acid monohydrate) buffer, 0.5 mol·m<sup>-3</sup> KCl, 0.5 mol·m<sup>-3</sup> MgCl<sub>2</sub>, 0.5 mol·m<sup>-3</sup> CaCl<sub>2</sub> (pH 5.7). A minor proportion of the cells at the surface of the bark strips was damaged by the pretreatment, as evidenced by the colouration after a 10-s immersion in 0.1% neutral red and subsequent rinsing in standard medium (Turgeon and Hepler 1989). The strips were mounted on microscope slides by clamping the ends of each strip under two lateral cover glasses which were fixed with Sellotape, and subsequently placed in a Perspex bathing chamber. The chamber, filled with standard medium, was mounted on the horizontal stage of an epifluorescence microscope (BH-2; Olympus Optical Instruments, Hamburg, FRG). During the experiment, the tissue was illuminated by the sub-stage microscope lamp.

**Measurement of the membrane potentials.** Glass microelectrodes with tip diameters less than 1 µm were fabricated from borosilicate microcapillaries with an inner filament (GC 150F-10; Clark Electromedical Instruments, Reading, UK) on a vertical electrode puller (Getra, München, FRG). To strengthen the electrode tip and to improve the electrical insulation of the tip, the microelectrodes were coated with polyvinylchloride (PVC). For coating, the tips (3 mm) of freshly prepared microelectrodes were hung in a PVC solution (0.15 g PVC per 1 ml tetrahydrofuran) for 15 min. In order to obtain a good PVC coating on the tip surface, a weak vacuum was created within the electrode through a syringe at the back end of the electrode. After the PVC coating had dried, the microelectrode was back-filled with 3 kmol·m<sup>-3</sup> LiCl.

Electrodes with a resistance of 20–60 MΩ were employed. The microelectrodes were clamped in Ag-AgCl pellet-holders (Clark Electromedical Instruments) and advanced by a motor-driven micromanipulator (Märzhäuser, Wetzlar, FRG). The pellet-holder of the measurement electrodes was connected to a custom-made microelectrode preamplifier with an input impedance of 10<sup>12</sup> Ω and a test pulse of 10<sup>-9</sup> A on the input. The reference electrode, connected to a ground lead, contained 3 kmol·m<sup>-3</sup> LiCl.

For impalement, easily accessible phloem areas were selected, where the target elements were covered by one to three layers of cells. Membrane sealing and stabilization of the membrane potential of sieve tubes required 10–20 min. Further details on the measuring equipment and the electrode impalement into sieve tubes in combination with iontophoresis have been given elsewhere (Van der Schoot and Van Bel 1989).

**Iontophoresis of Lucifer Yellow CH (LYCH).** Preparation of the tissues for E<sub>m</sub> measurement and iontophoresis was identical. In most experiments, the tips of the measurement electrodes were back-filled with approx. 10 µl 2% (w/v) LYCH source solution in water and filled up with 3 kmol·m<sup>-3</sup> LiCl. The presence of the dye increased the resistance of the electrode (up to 80 MΩ), but did not significantly affect the E<sub>m</sub> measurement (compare Van der Schoot and Van Bel 1989). After measurement of the E<sub>m</sub>, LYCH was iontophoretically injected by an intermittent (1 pulse·(10 s)<sup>-1</sup>) current injection of –15 to –25 nA (for 1–2 min). For current injection an extracellular preamplifier current pump (Dagan Corp., Minneapolis, Kan., USA) was used. After injection, the E<sub>m</sub> was remeasured to check the sealing of the protoplast and the electrode was carefully retracted. Injection and movement of the dye was observed continuously under blue light with an epifluorescence microscope equipped with the appropriate filter-set combination (excitation wavelength between 455 and 490 nm and a barrier filter of 495 nm). Most of the time, the blue light was dimmed to reduce the damaging effect of the light on the tissues. Photographs were taken with an Olympus OM-2 spot camera on Kodak Ektachrome 400 daylight film.

## Results

**Structure of the sieve tubes.** The main reason for using *Ricinus* and *Salix* stems was the relatively large diameter of the sieve tubes: this property facilitated the recognition of the sieve elements and made the impalement of microelectrodes less critical. An additional advantage is that the results can be readily related to the literature, as these species have been frequently employed in studies concerning phloem functioning along the path (e.g. *Ricinus* – Milburn 1970; Malek and Baker 1977; Vreugdenhil 1985; *Salix* – Weatherley et al. 1959; Sauter 1982; Peel and Rogers 1982; Peel 1987).

The sieve-element diameters in *Ricinus* stems were between 25 and 40 µm (Fig. 1E) which is in accordance with earlier observations (Milburn and Kallarackal 1984; Kallarackal and Milburn 1985), as were the values (16–25 µm; Fig. 1F) for *Salix* (Weatherley et al. 1959). The sieve elements of *Ricinus* are aligned in straight arrays and are separated by convexo-concave sieve plates with the convex face to the base-orientated side of the sieve tube (Fig. 1A, C, D, E). As has been pointed out before (Kallarackal and Milburn 1983), two types of sieve tubes were found: one with oblique sieve plates, the other with sieve plates perpendicular to the axis. The sieve elements of *Salix* adjoin more irregularly by oblique, gently S-shaped sieve plates (Fig. 1F).

**Plasmodesmata and plasmodesmatal frequencies.** The plasmodesmata between sieve elements and companion cells are branched, both in *Ricinus* and *Salix*. The branches are located, as usual, on the companion-cell side and are embedded in a small mound of wall material (Fig. 2A). In *Ricinus*, the diameter of the plasmodesma between sieve element and companion cell is 49 nm in the unbranched part, narrowing to 42 nm in the branches. Plasmodesmata between the phloem-parenchyma cells are mostly simple with sphincter-like constrictions, but branched plasmodesmata with a central cavity occur (Fig. 2B). The diameters of the plasmodes-

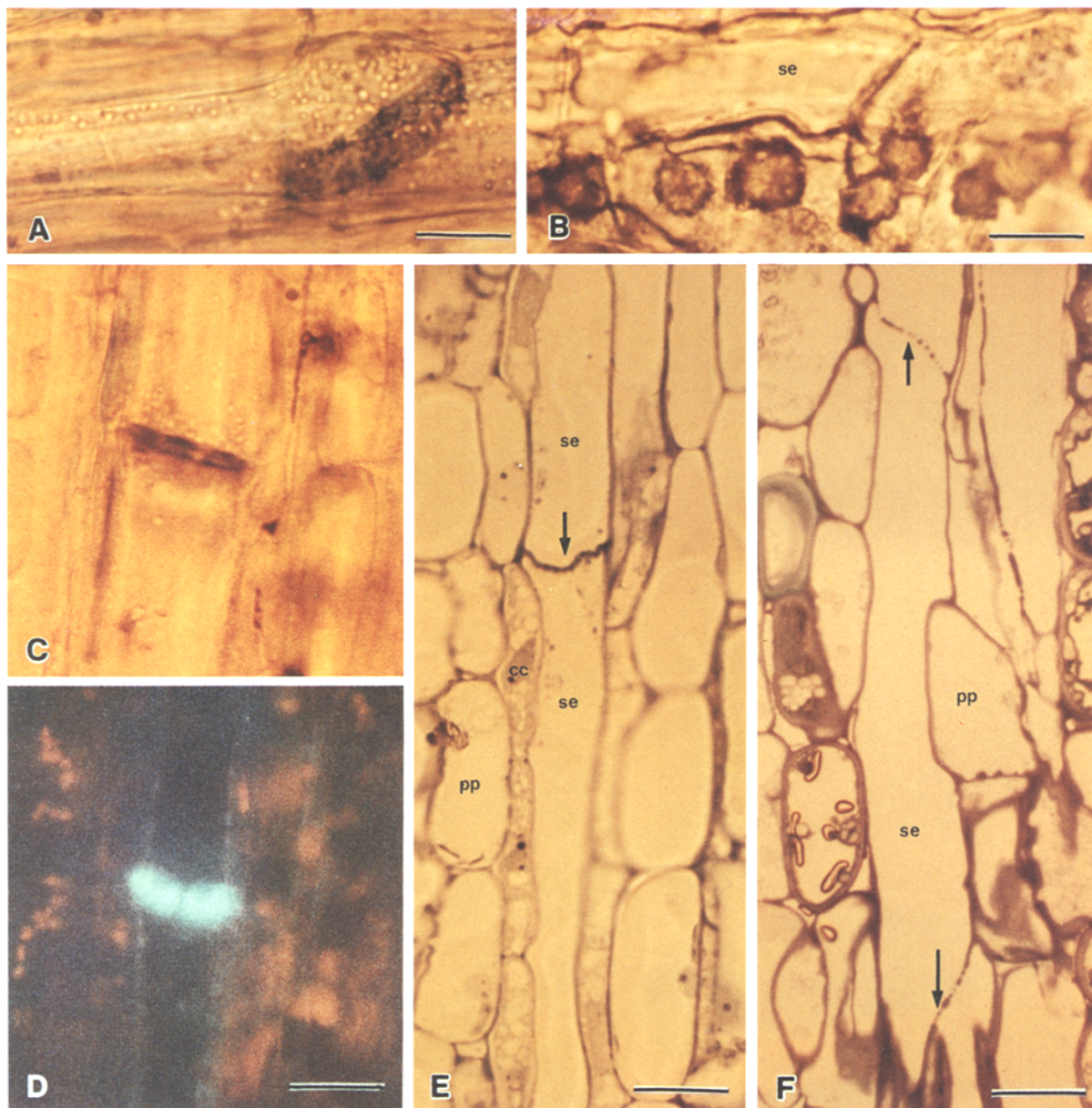


**Fig. 1A–F.** Localization of the sieve elements in phloem sections of *Ricinus* and *Salix* stems (all magnifications  $\times 550$ ; bar = 25  $\mu\text{m}$ ). **A** Fresh section of *Ricinus* phloem stained with aniline blue. The convexo-concave sieve plates are blueish, and the P-plastids are mainly located unilaterally against the sieve plate. **B** Phloem-parenchyma cells lining the sieve tubes of *Ricinus* and containing conspicuous spiny crystals. **C** Control picture for **D**. **D** *Ricinus* sieve plate

stained with aniline blue and viewed under ultraviolet light. **E** Section of *Ricinus* phloem showing a sieve plate (arrow). The lengths of the sieve elements are 360–500  $\mu\text{m}$ , the diameters, 20–40  $\mu\text{m}$ . **F** Section of *Salix* phloem showing sieve plates (arrows). The lengths of the sieve elements are 200–250  $\mu\text{m}$ , the diameters 16–25  $\mu\text{m}$

mata between the phloem-parenchyma cells were about 25 nm (Fig. 2C), both in *Salix* and *Ricinus*.

The plasmodesmatal frequencies between the phloem elements in *Ricinus* were counted by scanning ultrathin sections of the phloem area. The sections were scored every 4  $\mu\text{m}$  over a distance of 70  $\mu\text{m}$ , which is about one-fifth of the average sieve-element length. The plasmodesmatal frequency is expressed as the number of plasmodesmata per unit of stem length. This figure, representing absolute numbers of plasmodesmata, better quantifies the actual transport capacity of the plasmo-

desmata than relative values (i.e. plasmodesmata  $\cdot \mu\text{m}^{-2}$  of cell interface). The plasmodesmata between sieve tube-companion cell, sieve tube-phloem parenchyma, companion cell-phloem parenchyma and phloem parenchyma-phloem parenchyma were in the proportions 8:1:2:30, in the order given. The counting procedure was similar to that used for *Phaseolus* stem phloem (Hayes et al. 1985), with the difference that the branched plasmodesmata at the side of the companion cell were scored as a single unit. Branched plasmodesmata between the phloem-parenchyma cells were also counted

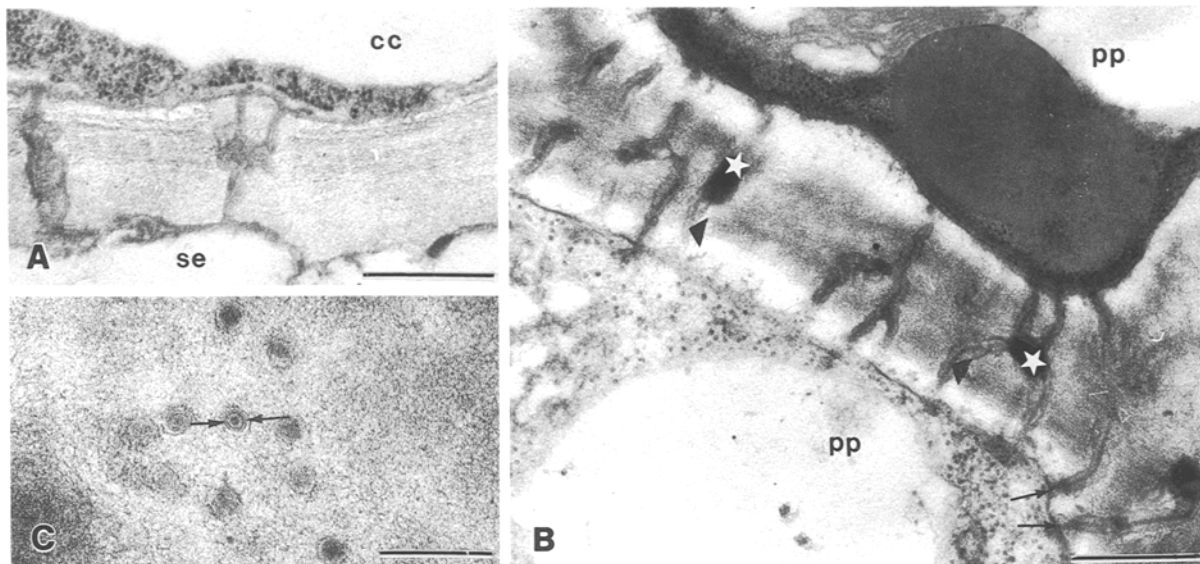


**Fig. 2A–C.** Ultrastructure of plasmodesmata between phloem elements. **A** Branched plasmodesma between sieve element and companion cell in *Ricinus* ( $\times 35600$ ; bar = 500 nm). The branches occur on the companion-cell side and are embedded in a mound of secondary cell-wall material. The diameter of the unbranched part is 49 nm, that of the branches 42 nm. **B** Branched plasmodesmata between phloem-parenchyma cells of *Salix* ( $\times 35600$ ; bar = 500 nm). Central cavities (asterisks), neck-constrictions (arrows) and central ER channel (arrowheads) are clearly visible. **C** Cross-section of plasmodesmata between phloem-parenchyma cells of *Salix* ( $\times 74400$ ; bar = 200 nm). The internal diameter of a plasmodesma (between the arrows) is 25–26 nm. The ER is visible in the centre of the plasmodesma

**Table 1.** Membrane potentials of se-cc complex and phloem parenchyma ( $\pm$  SD) after different ageing periods.  $n$  = number of measurements

	Membrane potential (mV)	
	1–6 h ageing	24–30 h ageing
<i>Ricinus communis</i>		
Se-cc complex	$-85.0 \pm 9.5$ ( $n=3$ )	— 90.0 ( $n=1$ )
Phloem parenchyma	$-44.5 \pm 7.9$ ( $n=10$ )	— 65.0 ( $n=2$ )
<i>Salix alba</i>		
Se-cc complex	— 65.0 ( $n=2$ )	$-127.7 \pm 5.9$ ( $n=3$ )
Phloem parenchyma	— 35.0 ( $n=2$ )	— 50.0 ( $n=1$ )

as a single plasmodesma. The plasmodesmal frequencies in *Salix* were not determined exactly, but again a symplastic constriction was apparent in the region between the se-cc complex and the phloem parenchyma.

**Membrane-potential measurements.** The three-dimensional structure of *Ricinus* phloem is more surveyable than that of *Salix* phloem and se-cc complexes are easier to trace. Sieve tubes in *Ricinus* were spotted by the rapidly vibrating P-plastids at either side of the sieve plates (Fig. 1A) and the sea-urchin-like crystals in adjacent

phloem-parenchyma cells (Fig. 1B). In *Salix*, the sieve plates were the only features that could be used to identify the sieve tubes (Fig. 1F).

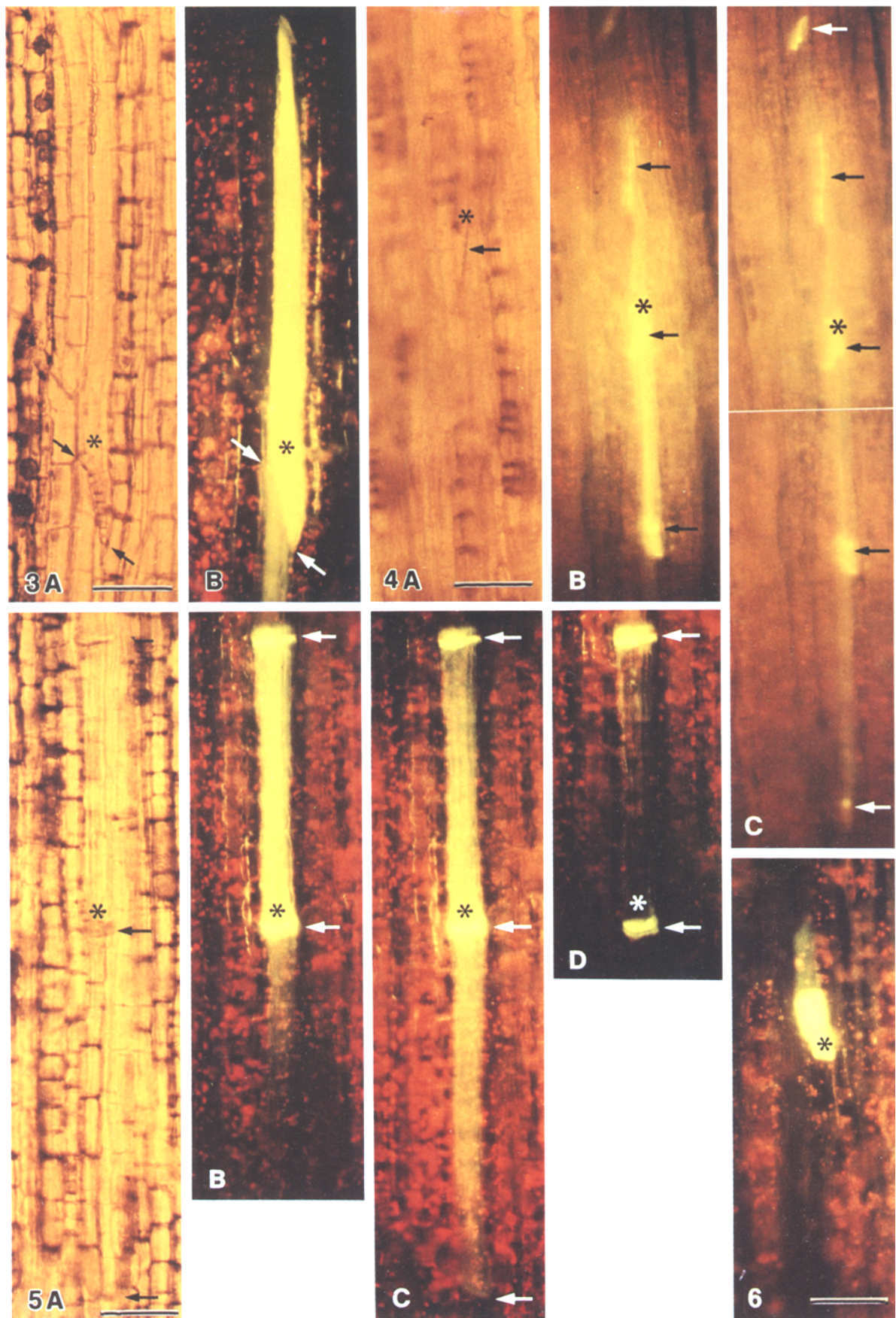
Membrane potentials of sieve tubes are extremely difficult to measure (compare Van Bel and Van der Schoot 1989), since the success rate of impalement is low. In tomato petioles, the high osmolarity of the sieve-tube content caused back-firing of the LYCH-electrolyte content of the electrode tip (Van der Schoot and Van Bel 1989). Back-firing of the fluorescent content in the electrode tip is observed when the electrode fluid is pushed back by the osmotic pressure of the sieve-tube

**Fig. 3A, B.** Movement of LYCH intracellularly injected into sieve tubes of *Ricinus*. **A** Control picture ( $\times 140$ ; bar = 100  $\mu\text{m}$ ) of LYCH-injected sieve tube (see **B**). The oblique sieve plate is marked by arrows. **B** Fluorescence micrograph of the sieve tube shown in **A**, 30 s after iontophoresis into the sieve element. The sieve plate is marked by arrows, the point of injection by an asterisk

**Fig. 4A–C.** Movement of LYCH intracellularly injected into sieve tubes of *Salix*. **A** Control picture ( $\times 140$ ; bar = 100  $\mu\text{m}$ ) of LYCH-injected sieve tube (see **B**). Sieve plates are marked by arrows. **B** Fluorescence micrograph of the sieve tube shown in **A**, 15 s after iontophoresis into the sieve element. Sieve plates are marked by arrows, the point of injection by an asterisk. **C** The same sieve tube 5 min after iontophoresis

**Fig. 5A–D.** Movement of LYCH intracellularly injected into sieve tubes of *Ricinus*. **A** Control picture ( $\times 140$ ; bar = 100  $\mu\text{m}$ ) of LYCH-injected sieve tube (see **B**). The transverse sieve plates are marked by arrows. **B** Fluorescence micrograph of the sieve tube shown in **A**, 15 s after iontophoresis into the sieve element. Sieve plates are marked by arrows, the point of injection by an asterisk. **C, D** The same sieve tube 1.5 and 10 min, respectively, after iontophoresis

**Fig. 6.** Displacement of LYCH intracellularly injected into a phloem-parenchyma cell of *Ricinus* ( $\times 140$ ; bar = 100  $\mu\text{m}$ ). The point of injection is marked by an asterisk. The micrograph was recorded 5 min after iontophoresis



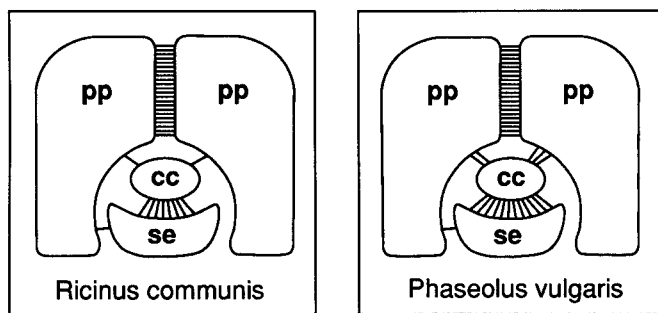


**Fig. 7.** Plasmodesmogram of the stem phloem of *Ricinus* and *Phaseolus*. The striping density represents the proportional number of plasmodesmata (plasmodesmata per unit of stem length) between the cell types. The plasmodesmogram of *Phaseolus* was reconstructed using the results of Hayes et al. (1985)

sap after impalement. In *Ricinus* and *Salix*, back-firing was not observed, indicating that the pressure in the sieve tubes as result of the osmopotential is not critical. The species-specific problems encountered here were the rigidity of the cell walls of *Salix* and the presumptive gelation of the sieve-tube contents of *Ricinus*.

Reliable recordings from se-cc complexes (Table 1) were scarce as a consequence of the problems mentioned above. Only the measurements that were stable for more than 10 min have been selected for Table 1. After each  $E_m$  measurement (Table 1), the cells were identified by dye-injection. Retention of the dye within the cytoplasmic compartments conformed with good sealing of the plasma membrane, as indicated by previous stability. The sealing makes considerable electrical leakage via the area impaled very unlikely. All measurements, both in fresh and in aged tissues, showed a spectacular jump in membrane potential between se-cc complex and phloem parenchyma (Table 1). The membrane potentials of the se-cc complex were generally twofold more negative than those of the phloem parenchyma. Such a difference in  $E_m$  between neighbouring cells can be maintained only if the symplastic connectivity is poor.

In *Ricinus*, the  $E_m$  values in fresh and aged tissues were similar. In contrast, the potential differences in *Salix* doubled after ageing, both in phloem parenchyma and the se-cc complex. Blind impalement, assumed to be into the se-cc complex of intact *Ricinus* plants, according to the method of Eschrich and coworkers (1988), yielded stable values of about  $-135$  mV.

**Iontophoresis of LYCH.** Labelling of the impaled cells by post-injection of LYCH by iontophoresis (compare Van der Schoot and Van Bel 1989), substantiated the claim that membrane potentials of sieve tubes had been recorded (Figs. 3–5). The exclusive luminiscence of the sieve-tube contents, in particular of their sieve plates, provided clear-cut evidence for that (Figs. 4, 5). Dye injected into a sieve tube remained restricted to the se-cc complex and moved in one direction immediately after iontophoresis and in the opposite direction after some minutes (Fig. 4B, C). The same often held for movement in *Ricinus* sieve tubes, but the series of photographs pre-

sented here (Fig. 5B–D) only shows unilateral movement of dye. Transfer of dye from sieve tube to companion cell was indicated by the fluorescence of the nuclei of the companion cells after 5–10 min (not shown).

Unlike those of *Salix*, the sieve plates in *Ricinus* exhibit differential fluorescence: the oblique plates are less fluorescent than the perpendicular ones (compare Figs. 3 and 5). Injection of dye into a companion cell resulted in transport to the sieve element. Both in *Salix* and *Ricinus*, iontophoresis of dye into phloem-parenchyma cells sometimes resulted in transfer to other phloem-parenchyma cells, but never in movement to the se-cc complex (Fig. 6).

## Discussion

The present investigations disclose structural and functional features consistent with symplastic autonomy of the se-cc complex. The plasmodesmatal frequencies between the phloem elements in *Ricinus* indicate a symplastic discontinuity between the se-cc complex and the phloem parenchyma. The symplastic isolation of the se-cc complex from the adjacent cells (Fig. 7) is illustrated by a plasmodesmogram which has been designed for immediate reading of plasmodesmatal configurations (compare Van Bel et al. 1988). A similar diagram reconstructed using the data for symplastic connectivity between the phloem elements in *Phaseolus* stems (Hayes et al. 1985), displays the same discontinuity (Fig. 7). Plasmodesmograms require critical use. Abundant connectivity does not necessarily imply intense intercellular traffic. Paucity of plasmodesmata inevitably indicates a constriction in the path between symplast units, but does not tell how quantitatively important this is.

The  $E_m$  values of the se-cc complex in *Ricinus* and *Salix* were more positive than the  $E_m$  measurements of the sieve-tube membranes of other species (Sibaoka 1962; Wright and Fisher 1981; Fromm and Eschrich 1988; Eschrich et al. 1988; Opritov and Pyatygyn 1989; Van der Schoot and Van Bel 1989). The most likely reason for the modest recordings is that the present studies were carried out with excised tissues, whilst previous measurements were mostly executed in intact plants either by use of cut aphid stylets (Fromm and Eschrich 1988) or by 'blind' impalement of excitable cells (Sibaoka 1962; Eschrich et al. 1988; Opritov and Pyatygyn 1989). Support for this conjection is that the  $E_m$  values for the se-cc complex of *Ricinus* were much higher using the 'blind' method ( $-135$  versus  $-90$  mV), and that the  $E_m$ 's of the se-cc complex in aged *Salix* tissue measured using glass electrodes ( $-127$  mV) and cut aphid stylets ( $-150$  to  $-160$  mV; Wright and Fisher 1981) are in the same order of magnitude.

The large difference in  $E_m$  between the se-cc complex and the surrounding cells (Table 1) has been also observed in *Mimosa* petioles (phloem parenchyma:  $-61$  mV, the likely se-cc complex:  $-161$  mV; Sibaoka 1962) and in tomato petioles (phloem parenchyma:  $-70$  mV, se-cc complex:  $-145$  mV) and stems (phloem parenchyma:  $-70$  mV, se-cc complex:  $-140$  mV; Van

der Schoot and Van Bel 1989). Despite the low absolute  $E_m$  values, the ratio of the  $E_m$ s of the se-cc complex and phloem parenchyma in *Salix* and *Ricinus* (Table 1) is similar to earlier results (Sibaoka 1962; Van der Schoot and Van Bel 1989). Since such dramatic differences between the  $E_m$  of the se-cc complex and those of the surrounding cells are explicable only if electric conductance is blocked, the  $E_m$ -jump seems to be a valid argument in favour of symplastic isolation of the se-cc complex.

Injection with LYCH unequivocally identified the impaled cells (Figs. 3–5) and implicitly demonstrated that  $E_m$  measurement of the se-cc complexes is feasible. Compared with the velocity in *Salix*, the movement of dye in *Ricinus* sieve tubes is slow. This may be a consequence of the high amount of P-proteins in *Ricinus* which probably causes gelation of the sieve-tube contents as a reaction to cutting (Alosi et al. 1988). The adhesion of LYCH to the sieve plates is the most conspicuous phenomenon of dye-labeling (Figs. 4, 5). The LYCH strongly attaches to aldehyde groups (Stewart 1981) which occur in glucans, the building blocks of callose (Kessler 1958). The fluorescence of the plates might therefore depend on the presence of callose. If this is true, then the oblique sieve plates (Fig. 3) of *Ricinus* contain little callose and this lack of callose formation could bring about the phloem bleeding of *Ricinus*. The presence of oblique and perpendicular sieve-plates in *Ricinus* (Figs. 3, 5), which has been observed before (Kallarackal and Milburn 1983), may point to a differential functioning of the sieve tubes.

It was noted before (Van der Schoot and Van Bel 1989, 1990) that plasmodesmata often shut off in response to excision of the tissue. Plasmodesmatal closure as result of wounding may thus explain the poor mobility of dye between the phloem-parenchyma cells which contrasts with the ready dye exchange between sieve tube and companion cell. The differential connectivity possibly results from differences in the ultrastructure of the plasmodesmata. The plasmodesmata between the phloem-parenchyma cells possess neck-constrictions (Fig. 2B) around the orifices. These organelles (Olesen 1979; Thomson and Platt-Aloia 1985) are presumed to react to changes in osmolarity (Zawadzki and Fensom 1986; Côté et al. 1987). In addition, the operational diameter of the plasmodesmata between the phloem parenchyma cells is much lower than 25 nm owing to the presence of a central rod (Fig. 2C), as has been amply discussed (Terry and Robards 1987). These properties sharply contrast with the absence of sphincters and the appreciable diameter (40–50 nm) of the symplastic connections between sieve tube and companion cell (Fig. 2).

It was speculated that the hydrodynamic plasmodesmatal properties change with the turgor relations between sieve tube and surrounding phloem parenchyma (Patrick 1990). Pressure-regulated plasmodesmatal valving between se-cc complex and phloem parenchyma would be consistent with this view. Such a temporary opening of the plasmodesmata would permit a flexible response to dramatic changes in stem metabolism. It is not excluded that some symplastic transport can occur

via the few plasmodesmata between the se-cc complex and the neighbouring parenchyma cells (Fig. 7) under the appropriate conditions. It has been claimed that under prevalent sink-limiting conditions, symplastic unloading of the sieve tube is possible (Hayes et al. 1987), but that unloading into the apoplast is the common mechanism of release. Permanent loss of photoassimilates into the apoplast demands steady retrieval by the se-cc complexes. This resorption is carrier-mediated (Maynard and Lucas 1982; Van Bel and Koops 1985; Daie 1987) and is, at least partly, driven by the proton-motive force. Exogenous application of sucrose provoked transient depolarization of the sieve-tube membrane potential (Wright and Fisher 1981; Van der Schoot and Van Bel 1989).

An efficient photoassimilate pump-leak system requires a high transmembrane transport capacity of the sieve tubes, in combination with symplastic isolation of the se-cc complex. Parachloromercuribenzenesulphonic acid (PCMBS) stimulated the release of sugars from the se-cc complex and inhibited that from the phloem parenchyma (Aloni et al. 1986). This differential susceptibility of the se-cc complex and the phloem parenchyma to PCMBS (Wolswinkel and Ammerlaan 1983; Aloni et al. 1986) conforms with a pump-leak system operating in symplastically isolated se-cc complexes.

We gratefully acknowledge the enthusiastic involvement in the experiments and the critical reading of the manuscript by Dr. C. van der Schoot (ATO, Wageningen). We thank Dr. F. Bretschneider (Laboratory of Animal Physiology, University of Utrecht) for helpful suggestions concerning the electronic set-up. The help of Dr. M. Erwee in preparation of the specimens of electron microscopy is highly appreciated. The hospitality of the Laboratory of Zoology (University of Utrecht) by providing electron-microscope facilities is greatly appreciated.

## References

- Aloni, B., Wyse, R.E., Griffith, S. (1986) Sucrose transport and phloem unloading in stem of *Vicia faba*: Possible involvement of a sucrose carrier and osmotic regulation. *Plant Physiol.* **81**, 482–486
- Alosi, M.C., Melroy, D.L., Park, R.B. (1988) The regulation of gelation of phloem exudate from *Cucurbita* fruit by dilution, glutathione, and glutathione reductase. *Plant Physiol.* **86**, 1089–1094
- Côté, R., Thain, J.F., Fensom, D.S. (1987) Increase in electrical resistance of plasmodesmata of *Chara* induced by an applied pressure gradient across nodes. *Can. J. Bot.* **65**, 509–511
- Daie, J. (1987) Sucrose uptake in isolated phloem of celery is a single saturable transport system. *Planta* **171**, 474–482
- Esau, K. (1973) Comparative studies of companion cells and phloem parenchyma cells in *Mimosa pudica* L. *Ann. Bot.* **37**, 625–632
- Eschrich, W., Fromm, J., Evert, R.F. (1988) Transmission of electric signals in sieve tubes of zucchini plants. *Bot. Acta* **101**, 327–331
- Fromm, J., Eschrich, W. (1988) Transport processes in stimulated and non-stimulated leaves of *Mimosa pudica*. II Energenesis and transmission of seismic stimulations. *Trees* **2**, 18–24
- Giaquinta, R.T. (1983) Phloem loading of sucrose. *Annu. Rev. Plant Physiol.* **34**, 347–387
- Hayes, P.M., Patrick, J.W. (1985) Photosynthate transport in stems

- of *Phaseolus vulgaris* L. treated with gibberellic acid, indole-acetic acid or kinetin. Effects at the site of hormone application. *Planta* **166**, 371–379
- Hayes, P.M., Offler, C.E., Patrick, J.W. (1985) Cellular structures, plasma membrane surface areas and plasmodesmatal frequencies of the stem of *Phaseolus vulgaris* L. in relation to radial photosynthate transfer. *Ann. Bot.* **56**, 125–138
- Hayes, P.M., Patrick, J.W., Offler, C.E. (1987) The cellular pathway of radial transfer in stems of *Phaseolus vulgaris* L.: Effects of cellular plasmolysis and *p*-chloromercuribenzenesulphonic acid. *Ann. Bot.* **59**, 635–642
- Kallarackal, J., Milburn, J.A. (1983) Studies on the phloem sealing mechanism in *Ricinus* fruit stalks. *Aust. J. Plant Physiol.* **10**, 561–568
- Kallarackal, J., Milburn, J.A. (1985) Phloem exudation in *Ricinus communis*: elastic responses and anatomical implications. *Plant Cell Environ.* **8**, 239–245
- Kessler, G. (1958) Zur Charakterisierung der Siebröhrenkallose. *Ber. Schweiz. Bot. Ges.* **68**, 5–43
- Malek, F., Baker, D.A. (1977) Proton co-transport of sugars in phloem loading. *Planta* **135**, 297–299
- Maynard, J.W., Lucas, W.J. (1982) Sucrose and glucose uptake into *Beta vulgaris* leaf tissues. A case for general (apoplastic) retrieval systems. *Plant Physiol.* **70**, 1436–1443
- Milburn, J.A. (1970) Phloem exudation from castor bean: induction by massage. *Planta* **95**, 272–276
- Milburn, J.A., Kallarackal, J. (1984) Quantitative determination of sieve-tube dimensions in *Ricinus*, *Cucumis* and *Musa*. *New Phytol.* **96**, 383–395
- Minchin, P.E.H., Thorpe, M.R. (1984) Apoplastic phloem unloading in the stem of bean. *J. Exp. Bot.* **35**, 538–550
- Minchin, P.E.H., Thorpe, M.R. (1987) Measurement of unloading and reloading of photoassimilate within the stem of bean. *J. Exp. Bot.* **38**, 211–220
- Minchin, P.E.H., Ryan, K.G., Thorpe, M.R. (1984) Further evidence of apoplastic unloading into the stem of bean: identification of the phloem buffering pool. *J. Exp. Bot.* **35**, 1744–1753
- Olesen, P. (1979) The neck-constriction in plasmodesmata. Evidence for a peripheral sphincter-like structure revealed by fixation with tannic acid. *Planta* **144**, 349–358
- Opritov, V.A., Pyatygina, S.S. (1989) Evidence for coupling of the action potential generation with the electrogenic component of the resting potential in *Cucurbita pepo* L. stem excitable cells. *Biochem. Physiol. Pflanz.* **184**, 447–451
- Patrick, J.W. (1990) Sieve element unloading: cellular pathway, mechanism and control. *Physiol. Plant.* **78**, 298–308
- Peel, A.J. (1987) Energy relations of solute loading in sieve elements of willow. *Planta* **172**, 290–213
- Peel, A.J., Rogers, S. (1982) Stimulation of sugar loading into sieve elements of willow by potassium and sodium salts. *Planta* **154**, 94–96
- Sauter, J.J. (1982) Transport in Markstrahlen. *Ber. Dtsch. Bot. Ges.* **95**, 593–618
- Sibaoka, T. (1982) Excitable cells in *Mimosa*. *Science* **137**, 226
- Stewart, W.W. (1981) Lucifer dyes – highly fluorescent dyes for biological tracing. *Nature* **292**, 17–21
- Terry, B.R., Robards, A.W. (1987) Hydrodynamic radius alone governs the mobility of molecules through plasmodesmata. *Planta* **171**, 145–157
- Thomson, W.W., Platt-Aloia, K. (1985) The ultrastructure of the plasmodesmata of the salt glands of *Tamarix* as revealed by transmission and freeze-fraction electron microscopy. *Protoplasma* **125**, 13–23
- Turgeon, R., Hepler, P.K. (1989) Symplastic continuity between mesophyll and companion cells in minor veins of *Cucurbita pepo* leaves. *Planta* **179**, 24–31
- Van Bel, A.J.E., Koops, A.J. (1985) Uptake of [<sup>14</sup>C]sucrose in isolated minor-vein networks of *Commelina benghalensis* L. *Planta* **164**, 362–369
- Van Bel, A.J.E., Van Kesteren, W.J.P., Papenhuijzen, C. (1988) Ultrastructural indications for coexistence of symplastic and apoplastic loading in *Commelina benghalensis* leaves. Differences in ontogenetic development, spatial arrangement and symplastic connections of the two sieve tubes in the minor vein. *Planta* **176**, 159–172
- Van der Schoot, C., Van Bel, A.J.E. (1989) Glass microelectrode measurements of sieve tube membrane potentials in internodes and petioles of tomato (*Solanum lycopersicum*). *Protoplasma* **149**, 144–154
- Van der Schoot, C., Van Bel, A.J.E. (1990) Mapping membrane potentials and dye coupling in internodal tissues of tomato (*Solanum lycopersicum* L.). *Planta* **182**, 9–21
- Vreugdenhil, D. (1985) Source-to-sink gradient of potassium in the phloem. *Planta* **163**, 238–240
- Weatherley, P.E., Peel, A.J., Hill, G.P. (1959) The physiology of the sieve tube. Preliminary investigations using aphid mouth parts. *J. Exp. Bot.* **10**, 1–16
- Wolswinkel, P., Ammerlaan, A. (1983) Sucrose and hexose release by excised stem segments of *Vicia faba* L.: The sucrose-specific stimulating influence of *Cuscuta* on sugar release and the activity of acid invertase. *J. Exp. Bot.* **34**, 1516–1527
- Wright, J.P., Fisher, D.B. (1981) Measurement of the sieve tube membrane potential. *Plant Physiol.* **67**, 845–848
- Zawadzki, T., Fensom, D.S. (1986) Transnodal transport of <sup>14</sup>C in *Nitella flexilis*. II Tandem cells with applied pressure gradient. *J. Exp. Bot.* **37**, 1353–1363